Thermal conductivity and interface thermal conductance of amorphous and crystalline Zr 47 Cu 31 Al 13 Ni 9 alloys with a Y 2 O 3 coating

Nitin C. Shukla, Hao-Hsiang Liao, Jeremiah T. Abiade, Fengxiao Liu, Peter K. Liaw, and Scott T. Huxtable

Citation: Applied Physics Letters **94**, 081912 (2009); doi: 10.1063/1.3090487
View online: http://dx.doi.org/10.1063/1.3090487
View Table of Contents: http://scitation.aip.org/content/aip/journal/apl/94/8?ver=pdfcov
Published by the AIP Publishing

Thermal conductivity and interface thermal conductance of amorphous and crystalline $Zr_{47}Cu_{31}Al_{13}Ni_9$ alloys with a Y_2O_3 coating

Nitin C. Shukla,[1] Hao-Hsiang Liao,[1] Jeremiah T. Abiade,[1,2] Fengxiao Liu,[3] Peter K. Liaw,[3] and Scott T. Huxtable[1,a)]

[1]*Department of Mechanical Engineering, Virginia Polytechnic Institute and State University, Blacksburg, Virginia 24061, USA*

[2]*Department of Materials Science and Engineering, Virginia Polytechnic Institute and State University, Blacksburg, Virginia 24061, USA*

[3]*Department of Materials Science and Engineering, The University of Tennessee, Knoxville, Tennessee 37996, USA*

(Received 7 October 2008; accepted 8 February 2009; published online 27 February 2009)

We examine the thermal conductivity k and interface thermal conductance G for amorphous and crystalline $Zr_{47}Cu_{31}Al_{13}Ni_9$ alloys in contact with polycrystalline Y_2O_3. Using time-domain thermoreflectance, we find $k=4.5$ W m^{-1} K^{-1} for the amorphous metallic alloy of $Zr_{47}Cu_{31}Al_{13}Ni_9$ and $k=5.0$ W m^{-1} K^{-1} for the crystalline $Zr_{47}Cu_{31}Al_{13}Ni_9$. We also measure $G=23$ MW m^{-2} K^{-1} for the metallic glass/Y_2O_3 interface and $G=26$ MW m^{-2} K^{-1} for the interface between the crystalline $Zr_{47}Cu_{31}Al_{13}Ni_9$ and Y_2O_3. The thermal conductivity of the crystalline Y_2O_3 layer is found to be $k=5.0$ W m^{-1} K^{-1}, and the conductances of Al/Y_2O_3 and Y_2O_3/Si interfaces are 68 and 45 MW m^{-2} K^{-1}, respectively. © *2009 American Institute of Physics*. [DOI: 10.1063/1.3090487]

As the feature size of modern electronic devices continues to decrease, the influence of interfaces on heat transfer becomes increasingly important. With layer thicknesses typically in the range of tens to hundreds of nanometers, the interface thermal resistance can often dominate over the thermal resistances intrinsic to the layers themselves. In many instances, heat must be transferred from metallic layers to nonmetallic layers, thus better understanding of the flow of heat between metals and nonmetals would lead to improved thermal management and enhanced overall performance in electronic devices.

The flow of heat from a metal to a nonmetal requires that the energy carried by the electrons in the metal be transferred to the lattice of the nonmetal where thermal energy is carried in the form of lattice vibrations (phonons). This energy can (a) be transferred directly from the electrons in the metal to the lattice of the nonmetal, or (b) it may first be transferred from the electrons in the metal to the lattice of the metal and then to the nonmetal via phonon-phonon coupling at the interface.[1] The relative importance of each of these two pathways has remained difficult to assess experimentally. In this work, we examine the thermal conductivity and interface thermal conductance of amorphous and crystalline metallic alloys of $Zr_{47}Cu_{31}Al_{13}Ni_9$ in contact with polycrystalline Y_2O_3. By changing the structure, but not the composition, of the alloys, we aim to gain some insight into the role of the metallic lattice on the interface thermal conductance as well as thermal conductivity of these materials.

In the amorphous form, metallic alloys are often known as bulk metallic glasses (BMGs), and they exhibit great strength, hardness, toughness, corrosion resistance, and elasticity.[2–7] For example, BMGs may possess twice the strength to weight ratio of steels, and they are tougher yet more elastic than ceramics. Their unique properties have led to the use of BMG in a variety of applications, such as linear actuators, fuel-cell separators, aircraft parts, and sporting goods.[8] In addition to their amorphous glass form, these metallic alloys can often be fabricated in a crystalline form if they are cooled slowly during casting.

The amorphous and crystalline $Zr_{47}Cu_{31}Al_{13}Ni_9$ samples are prepared by arc melting a mixture of the constituent metals of Zr, Cu, Al, and Ni (>99.9% in purity) in a Ti-gettered argon atmosphere. To ensure a homogeneous distribution of the chemical elements, the ingot is melted and flipped three times. The glassy alloy is fabricated using a copper-mold casting method. The amorphous substrates are produced from cylindrical rods that are 4 mm in diameter and 50 mm in length. The crystalline $Zr_{47}Cu_{31}Al_{13}Ni_9$ ingots are melted in the same condition and are cooled slowly. Polycrystalline Y_2O_3 films are deposited on the metallic alloys by pulsed laser deposition at 400 °C.

The thermal conductivity and interface thermal conductance of the samples are found using time-domain thermoreflectance (TDTR).[9,10] TDTR is a pump-probe optical technique that takes advantage of the fact that the reflectance of a metal depends slightly on temperature. A laser pulse with a wavelength of 800 nm is split into two beams, and the modulated pump beam is used to heat the sample. The time-delayed probe beam reflects off an aluminum layer that coats the surface of the sample and into a photodetector, giving a measure of the temperature decay at the surface since the reflectivity of aluminum depends on temperature. Lock-in amplifiers measure the in-phase and out-of-phase signals from the photodetector. The thermal conductivity and interface thermal conductance are extracted simultaneously by comparing the experimental data to a thermal model and adjusting the two parameters until the model matches the data.[11] The inputs to the model include the thickness, heat capacity, and thermal conductivity for each layer in the sample. Interfaces are treated as thin layers (1 nm thick) where the conductance is given by the ratio of the thermal

a)Electronic mail: huxtable@vt.edu.

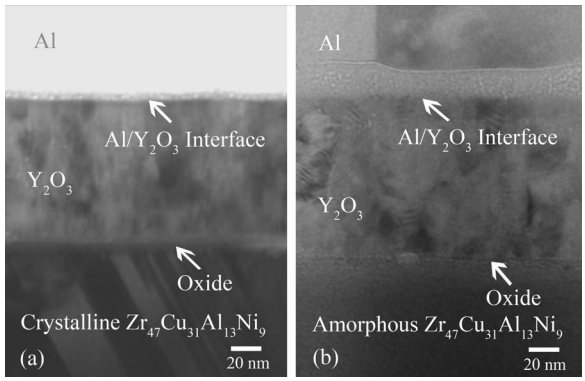

FIG. 1. TEM micrographs of (a) crystalline $Zr_{47}Cu_{31}Al_{13}Ni_9$ with Y_2O_3 and Al and (b) amorphous $Zr_{47}Cu_{31}Al_{13}Ni_9$ with Y_2O_3 and Al. Note the presence of a ~5 nm thick oxide layer on the surface of metallic alloy layers. The lack of structure in the Al layer and the blurriness of the entire image in (a) is an artifact due to the unfortunately large thickness of the TEM specimen. The TEM specimen for sample (b) is considerably thinner, thus the image is sharper. The change in structure in the Al layer in (b) after ~20 nm is likely due to a sudden change in the deposition rate of the Al during electron beam evaporation. The two blocks at the top of the Al layer are crystallites. Energy dispersive x-ray spectroscopy analyses on both aluminum layers confirm that the entire layers are essentially pure aluminum. The change in structure of the aluminum throughout the layer should have minimal effect on our results since the heat capacity and thermal conductivity of aluminum are not significantly influenced by these changes in morphology.

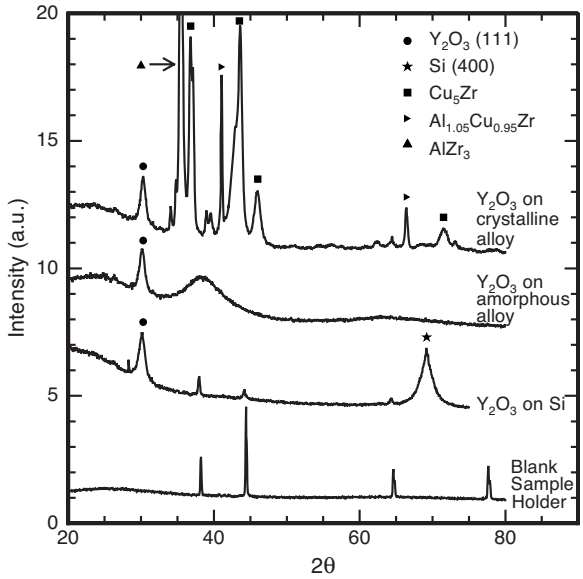

FIG. 2. XRD patterns for Y_2O_3, amorphous and crystalline $Zr_{47}Cu_{31}Al_{13}Ni_9$ alloys, and Si. The XRD patterns are obtained using *K*-alpha emission from copper with a wavelength of 1.5406 Å. The sharp peaks for Y_2O_3 and one alloy indicate that the materials are partially crystalline, while the broad peak for the second alloy demonstrates that it is amorphous. The labels on the plot refer to peaks that are matched with materials in the Powder Diffraction File database (PDF). The sharp peaks that appear in the blank sample holder are partially attenuated in the Y_2O_3 on Si sample, and fully attenuated in the metallic alloy samples due to the increased thickness of these samples.

conductivity to the heat capacity for the layer.

The overall structures of the samples of interest consist of the metallic alloy substrate (~1 mm thick), followed by a Y_2O_3 layer (~95 nm thick) that is coated with a reflective aluminum layer (~80 nm thick). Transmission electron microscopy (TEM) images of the Al/Y_2O_3/alloy structures are shown in Fig. 1, and x-ray diffraction (XRD) patterns appear in Fig. 2. The XRD results in Fig. 2 confirm that a polycrystalline Y_2O_3 layer was deposited on both metallic alloy substrates and that one metallic alloy was amorphous while the other was crystalline. Before we can extract the thermal conductivity of the metallic alloy and the conductance of the alloy/Y_2O_3 interface, we first need to find the thermal conductivity k for the Y_2O_3 layer and the interface thermal conductance G for the Al/Y_2O_3 interface by examining a separate reference sample.

Thus, we first prepare a sample consisting of a silicon wafer coated with polycrystalline Y_2O_3 (Fig. 2) and aluminum. We determine the thermal conductivity of the aluminum to be $k=190$ W m^{-1} K^{-1} with four-point probe measurements of the electrical conductivity in conjunction with the Wiedemann–Franz law. We use literature values for the thermal conductivity of Si,[12] and the heat capacities of Si,[12] Al,[13] and Y_2O_3.[14] The thickness of the Al (~82 nm) and Y_2O_3 (~73 nm) layers are found from acoustic echoes[15] with speeds of sound of 6420 m/s for Al (Ref. 13) and 7000 m/s for Y_2O_3.[16,17] These thickness measurements are confirmed with TEM. With a laser modulation frequency of $f=9.86$ MHz, we find $k=5$ W m^{-1} K^{-1} for the Y_2O_3, $G=68$ MW m^{-2} K^{-1} for the Al/Y_2O_3 interface, and $G=45$ MW m^{-2} K^{-1} for the Y_2O_3/Si interface. The thermal conductivity of the thin Y_2O_3 layer is about a factor of 5 smaller than a reported value of $k=27$ W m^{-1} K^{-1} for a bulk Y_2O_3 crystal.[18]

Next we turn our attention back to our Al/Y_2O_3/metallic alloy samples. The heat capacity of the $Zr_{47}Cu_{31}Al_{13}Ni_9$ alloy is calculated to be $C=2.24$ J cm^{-3} K^{-1} using the Kopp–Neumann law. This calculated value is close to an experimentally determined value[19] of $C=2.28$ J cm^{-3} K^{-1} for a similar metallic glass, $Zr_{55}Cu_{30}Al_{10}Ni_5$. In order to confirm our results and to increase the sensitivity of the measurements, we examine the Al/Y_2O_3/alloy samples at modulation frequencies of $f=9.86$ MHz and $f=4.77$ MHz. Since the penetration depth of the thermal wave is inversely proportional to the square root of the modulation frequency, the lower frequency gives us better sensitivity to the Y_2O_3/alloy interface that is buried deeper in the sample, while the higher frequency measurements allow us to confirm our previous measurements for k of the Y_2O_3 layer and G for the Al/Y_2O_3 interface. Thermoreflectance data are shown in Fig. 3 along with "best-fit" curves from the thermal model.

From the TDTR measurements, we find that $k=4.5$ W m^{-1} K^{-1} for the amorphous alloy, and $k=5.0$ W m^{-1} K^{-1} for the crystalline alloy. These thermal conductivity values are similar to those reported by Yamasaki *et al.* for amorphous $Zr_{55}Al_{10}Ni_5Cu_{30}$ (Ref. 19, 5.0 W m^{-1} K^{-1}) and for amorphous $Zr_{41}Ti_{14}Cu_{12}Ni_{10}Be_{23}$ (Ref. 20, 4.6 W m^{-1} K^{-1}). We can estimate the electronic contribution k_e to each thermal conductivity value by again using the Wiedemann–Franz law in conjunction with the Van der Pauw method for electrical conductivity measurements. We find $k_e=3.75$ W m^{-1} K^{-1} for the amorphous alloy and $k_e=4.0$ W m^{-1} K^{-1} for the crystalline alloy, which leaves lattice (phonon) components k_p of the thermal conductivity of $k_p=0.75$ W m^{-1} K^{-1} for the amorphous alloy and $k_p=1.0$ W m^{-1} K^{-1} for the crystalline alloy. As a point of comparison, we calculate the minimum lattice thermal conductivity[21] using material properties for a similar

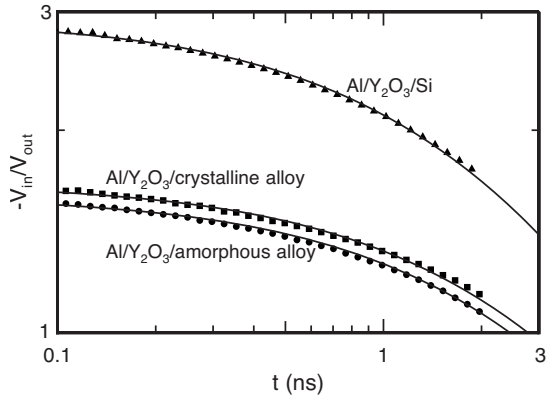

FIG. 3. TDTR on the Al/Y_2O_3/alloys and the $Al/Y_2O_3/Si$ sample. V_{in}/V_{out} represents the ratio of the in-phase/out-of-phase voltage as measured by a lock-in amplifier. The data taken on the $Al/Y_2O_3/Si$ sample (▲) are used to find the conductivity of the Y_2O_3 layer as well as the conductance of the Al/Y_2O_3 and Y_2O_3/Si interfaces. The measurements on the crystalline (■) and amorphous (●) alloys give the conductivity of each alloy along with the conductance of each Y_2O_3/alloy interface. The solid lines represent the best-fit from the thermal model. The models all used identical material properties for Al, the Al/Y_2O_3 interface, and the Y_2O_3 layer.

$(Zr_{55}Cu_{30}Al_{10}Ni_5)$ BMG (Ref. 22) and find $k_{min}=0.6$ W m^{-1} K^{-1}.

Finally, we extract the interface thermal conductance between the alloy and Y_2O_3 layer and find $G=23$ MW m^{-2} K^{-1} for the amorphous alloy/Y_2O_3 interface and $G=26$ MW m^{-2} K^{-1} for the crystalline alloy/Y_2O_3 interface. We also point out that there is a ~5 nm thick oxide layer present at the alloy/Y_2O_3 interfaces as is typical of Zr-based BMG.[23] Thus, our reported interface conductance is really the sum of the interface conductance between the Y_2O_3 and the oxide, the conductance of the oxide layer itself, and the interface conductance between the oxide and the metallic alloy. However, if we assume a typical oxide conductivity of 1 W m^{-1} K^{-1} for this layer, the oxide layer itself would only contribute ~12% of the total thermal resistance of the interface. Thus, the transfer of energy between the metal and nonmetal dominates the measured interface conductance. While part of the motivation for this study was to examine the effect of the alloy structure on the interface conductance, it is difficult to draw solid conclusions about the precise role of electron-phonon or phonon-phonon coupling at the interface due to the small separation in the lattice components of the thermal conductivity of the amorphous and crystalline layers. Future work will focus on materials that possess a larger difference in lattice thermal conductivity between crystalline and amorphous structures.

This work was partially supported by the United States National Science Foundation (U.S. NSF) under Grant No. CBET-0547122 and by the Thomas F. and Kate Miller Jeffress Memorial Trust under Grant No. J-799. Some of this work was carried out using instruments in the Nanoscale Characterization and Fabrication Laboratory, a Virginia Tech facility operated by the Institute for Critical Technology and Applied Science, and we thank W. Reynolds, J. McIntosh, and M. Murayama for their assistance with structural characterizations. F.L. and P.K.L. are grateful to the U.S. NSF for the following support: (1) The Combined Research-Curriculum Development (CRCD) Program, under Grant Nos. EEC-9527527 and EEC-0203415, Ms. M. Poats; (2) The Integrative Graduate Education and Research Training (IGERT) Program, under Grant No. DGE-9987548, Dr. C. J. Van Hartesveldt, Dr. D. Dutta, Dr. W. Jennings, and Dr. L. Goldberg; and (3) The International Materials Institutes (IMI) Program, under Grant No. DMR-0231320, Dr. C. Huber.

[1] A. Majumdar and P. Reddy, Appl. Phys. Lett. **84**, 4768 (2004).
[2] M. Telford, Mater. Today **7**, 36 (2004).
[3] C. J. Byrne and M. Eldrup, Science **321**, 502 (2008).
[4] A. L. Greer and E. Ma, MRS Bull. **32**, 611 (2007).
[5] W. L. Johnson, MRS Bull. **24**, 42 (1999).
[6] M. Miller and P. K. Liaw, *Bulk Metallic Glasses* (Springer, New York, 2007).
[7] M. L. Morrison, R. A. Buchanan, A. Peker, P. K. Liaw, and J. A. Horton, J. Non-Cryst. Solids **353**, 2115 (2007).
[8] I. Inoue and N. Nishiyama, MRS Bull. **32**, 651 (2005).
[9] D. G. Cahill, W. K. Ford, K. E. Goodson, G. D. Mahan, A. Majumdar, H. J. Maris, R. Merlin, and S. R. Phillpot, J. Appl. Phys. **93**, 793 (2003).
[10] S. Huxtable, D. G. Cahill, V. Fauconnier, J. O. White, and J.-C. Zhao, Nature Mater. **3**, 298 (2004).
[11] D. G. Cahill, Rev. Sci. Instrum. **75**, 5119 (2004).
[12] H. R. Shanks, P. D. Maycock, P. H. Sidles, and G. C. Danielson, Phys. Rev. **130**, 1743 (1963).
[13] D. R. Lide, *CRC Handbook of Chemistry and Physics*, 82nd ed. (Chemical Rubber Company, Boca Raton, Florida, 2002).
[14] V. Swamy, H. J. Seifert, and F. Aldinger, J. Alloys Compd. **269**, 201 (1998).
[15] H. T. Grahn, H. J. Maris, and J. Tauc, IEEE J. Quantum Electron. **25**, 2562 (1989).
[16] J. W. Palko, W. M. Kriven, S. V. Sinogeikin, J. D. Bass, and A. Sayir, J. Appl. Phys. **89**, 7791 (2001).
[17] C. Proust, Y. Vaills, Y. Luspin, and E. Husson, Solid State Commun. **93**, 729 (1995).
[18] P. H. Klein and W. J. Croft, J. Appl. Phys. **38**, 1603 (1967).
[19] M. Yamasaki, S. Kagao, and Y. Kawamura, Scr. Mater. **53**, 63 (2005).
[20] M. Yamasaki, S. Kagao, Y. Kawamura, and K. Yoshimura, Appl. Phys. Lett. **84**, 4653 (2004).
[21] D. G. Cahill, S. K. Watson, and R. O. Pohl, Phys. Rev. B **46**, 6131 (1992).
[22] T. Mashimo, H. Togo, Y. Zhang, Y. Uemura, T. Kinoshita, M. Kodama, and Y. Kawamura, Appl. Phys. Lett. **89**, 241904 (2006).
[23] U. Köster and L. Jastrow, Mater. Sci. Eng., A **449**, 57 (2007).